Kinetic Alfvén waves generated by ion beam and velocity shear in the Earth's magnetosphere

View Online   Export Citation   CrossMark

K. C. Barik,[a) iD] S. V. Singh,[b) iD] and G. S. Lakhina[c)]

AFFILIATIONS

Indian Institute of Geomagnetism, Navi Mumbai 410218, India

[a)]Electronic mail: kcbarik16@iigs.iigm.res.in
[b)]Electronic mail: satyavir@iigs.iigm.res.in
[c)]Electronic mail: gslakhina@gmail.com

ABSTRACT

Generation of Kinetic Alfvén Waves (KAWs) in a generalized three component plasma model consisting of the background cold ions, hot electrons, and hot ion beams, where all the three species have non-uniform streaming and velocity shear, is discussed. First, the role played by the ion beam solely in exciting KAWs is analyzed. Next, how this behavior gets modified when the velocity shear is present along with the streaming ion beam is discussed. The effects of other parameters such as temperature, number density, and propagation angle on the growth of KAWs are explored. It is found that when shear is positive and ions are streaming along the ambient magnetic field, KAWs are stabilized. On the other hand, with positive shear and an anti-parallel ion beam or vice-versa, KAWs with a larger growth rate are excited as compared to the case of waves excited by the ion beam alone. Also, for the first time, we have shown the combined effect of the ion beam and velocity shear on the generation of KAWs. The theoretical model can generate ultra-low frequency waves with frequencies up to ≈60 mHz for the plasma parameters relevant to auroral/ polar cusp field lines.

Published under license by AIP Publishing. https://doi.org/10.1063/1.5065461

I. INTRODUCTION

Ultra-low frequency (ULF) waves, in the frequency range of ∼0–30 Hz, have been widely observed in various regions of the Earth's magnetosphere, e.g., magnetopause, magnetosheath, plasma sheet boundary layer, polar cusp, and on auroral field lines.[1–14] Various mechanisms have been proposed for the generation of these ULF waves, e.g., by Kelvin-Helmholtz (K-H) instability[1,15–17] and Kinetic Alfvén Waves (KAWs).[18–26] Kinetic Alfvén Waves (KAWs) are ultra-low frequency electromagnetic waves which propagate nearly perpendicular to the ambient magnetic field and play a major role in the particle energization and acceleration of electrons. The parallel component of the electric field associated with the KAWs is responsible for the particle acceleration along the ambient magnetic field.[24,27] The kinetic Alfvén waves cannot exist in ideal MHD conditions; both electrons and ions need to be treated as separate fluid (two fluid approach). Primarily, the kinetic effects appear in the Alfvén waves under two conditions: First, in the hot electron plasma, when the perpendicular wavelength is comparable to the ion gyroradius.[18] Second, in the cold electron plasma, when the perpendicular wavelength is comparable to the electron inertial length.[19] Generally, these two effects are included in the description of the kinetic Alfvén waves which produce parallel electric field and have been widely used in the literature. However, Alfvén waves can also have parallel electric fields produced by the mirror effect[28] which can be larger than the electric field produced by finite Larmor or inertial effects. Such waves are called mirror kinetic Alfvén waves. However, it will require an inhomogeneous magnetic field. Various satellites have observed kinetic Alfvén waves at the magnetopause,[29–31] in the plasma sheet,[10,32] at the geostationary orbit,[33,34] in the inner magnetosphere,[35–38] in the auroral zone,[39–41] and in the solar wind.[42] The importance of linear and nonlinear kinetic Alfvén waves in localization and generation of turbulence in various regions of the Earth's magnetosphere has been extensively studied.[43–47]

Lakhina[26] proposed velocity shear instability as a possible generation mechanism for the ULF waves and explained how the velocity shear can excite the KAWs and showed that the

frequency of the KAWs is in the range of ULF waves. Though the theory developed was a generalized one including ion beams and velocity shear, the results presented in the paper were confined to the generation of kinetic Alfvén waves by velocity shear only. In this paper, the work of Lakhina[26] is extended to study the generation of KAWs by ion beams and also with the combined sources of ion beam and velocity shear. The theoretical model comprises cold background ions, hot electrons, and hot ion beams, where all the three components have the Maxwellian distribution and all have non-uniform streaming and velocity shear. The plasma is immersed in a homogeneous magnetic field and considers finite Larmor radius effects. Here, we will discuss the resonant instability. The effect of physical parameters such as the number density, the temperature of the plasma species, and the propagation angle will be examined. This paper is organized as follows: in Sec. II, the theoretical model for KAWs is presented. In Sec. III, the dispersion relation is derived and analysed for resonant instability. The results are concluded in Sec. IV.

II. THEORETICAL MODEL FOR KAWs EXCITED BY THE ION BEAM

We consider a three-component plasma model[26] consisting of electrons (N_e, T_e), background ions [protons, (N_i, T_i)], and ion beam (N_B, T_B) in a uniform magnetic field $\mathbf{B}_0 = B_0\hat{z}$. We keep the theoretical model very general where all the three plasma species can have non-uniform streaming velocity, $\mathbf{V}_j = V_j(X)\hat{z}$, where $X = x + v_y/\omega_{cj}$ and $\omega_{cj} = (e_j\mathbf{B}_0/cm_j)$ is the gyro-frequency of the jth species, where the subscripts $j = e$, i, and B represent the electrons, background ions, and beam ions, respectively. Furthermore, e_j and m_j are the charge and mass of the jth species and c is the velocity of light. It means that all the particles can stream along the Z-direction, i.e., along the background magnetic field, whereas they have the gradient along the x-direction perpendicular to the direction of streaming. Furthermore, N_j and T_j represent the number density and temperature of the jth plasma species. The charge neutrality condition in the equilibrium is given by the relation $N_e = N_i + N_B$. Since we are considering low-frequency waves driven by velocity shear, the equilibrium distribution is assumed of the form

$$f_{0j} = (\pi\alpha_j^2)^{-3/2}N_j \exp\left[-(v_\perp^2 + (v_\parallel - V_j(X))^2)/\alpha_j^2\right], \quad (1)$$

where $v_\perp = \sqrt{v_x^2 + v_y^2}$, and $v_\parallel = v_z$ are the perpendicular and parallel velocity components, respectively, and $\alpha_j = (2T_j/m_j)^{1/2}$ is the thermal speed of the jth species.

Since the kinetic Alfvén wave (KAW) is an electromagnetic wave, it is better to write the wave electric field $\mathbf{E}$ as the gradient of two scalar potentials ϕ and ψ such that

$$\mathbf{E} = -\nabla_\perp\phi + E_\parallel\hat{z}, \quad (2)$$

where parallel and perpendicular components of the electric field can be expressed as $E_\parallel = -\nabla_\parallel\psi$ and gradient of scalar potential ϕ. Poisson's equation for kinetic Alfvén waves can be written as

$$-\nabla_\perp^2\phi + \frac{\partial E_\parallel}{\partial z} = 4\pi\sum_j e_j n_j, \quad (3)$$

and the expression for the parallel component of Ampère's law is given by

$$\frac{\partial\nabla_\perp^2\phi}{\partial z} + \nabla_\perp^2 E_\parallel = \frac{4\pi}{c^2}\frac{\partial}{\partial t}\sum_j \mathbf{J}_{zj}. \quad (4)$$

Here, n_j and $\mathbf{J}_{zj}$ represent the perturbed number and the z-component of the current densities, respectively, and can be estimated by the following expressions:

$$n_j = \int d^3 v f_{1j},$$
$$\mathbf{J}_{zj} = \int d^3 v e_j v_z f_{1j}, \quad (5)$$

where f_{1j} is the perturbed distribution function. In order to obtain the perturbed distribution function from the linearized Vlasov's equation, the perturbation is assumed to be of the form $f_{1j} = \exp(ik_\perp y + ik_\parallel z - i\omega t)$, where ω is the frequency of the wave, and $k_\parallel$ and $k_\perp$ are the parallel and perpendicular components of the wave vector $\mathbf{k}$, respectively. Here, we restrict our perpendicular wave vector to the y-direction and use a local approximation ($L_j k \gg 1$) to solve linearized Vlasov's equation. Here, k is the wave number and $L_j = V_j(dV_j/dx)^{-1}$ is the velocity gradient scale length. Thus, the generalized perturbed distribution function can be written as[57]

$$f_1(\mathbf{r},\mathbf{v},t) = -\frac{q}{m}\int_{-\infty}^t dt'\left[1 + \frac{(\mathbf{E}\cdot\mathbf{v}')\mathbf{k} - \mathbf{E}(\mathbf{v}'\cdot\mathbf{k})}{\omega}\right]$$
$$\cdot\nabla_{v'}f_0(\mathbf{v}')e^{i(\mathbf{k}\cdot\mathbf{r}'-\omega t')}, \quad (6)$$

which has to be integrated along the trajectories, $\mathbf{r}(\mathbf{r}',\mathbf{v}',t')$, which ends at $\mathbf{r}(\mathbf{r},\mathbf{v},t)$ when $t' = t$. Following the standard procedure and algebraic manipulations, the perturbed distribution function for low-frequency kinetic Alfvén waves can be written as

$$f_{1j} = \frac{e_j}{m_j}\sum_{n=-\infty}^{+\infty}\sum_{m=-\infty}^{+\infty}\frac{e^{i(n-m)\theta}}{(k_\parallel v_z - \omega + n\omega_{cj})}J_n(\xi_j)J_m(\xi_j)$$
$$\times(k_\perp M_j\phi + k_\parallel L_j\psi), \quad (7)$$

where coefficients M_j and L_j can be expressed as

$$M_j = \left(1 - \frac{k_\parallel v_z}{\omega}\right)\left[\frac{\partial f_{0j}}{\partial v_\perp}\cdot\frac{n\omega_{cj}}{k_\perp v_\perp} + \frac{1}{\omega_{cj}}\cdot\frac{\partial f_{0j}}{\partial x}\right] + \frac{\partial f_{0j}}{\partial v_z}\frac{n\omega_{cj}k_\parallel}{k_\perp\omega}, \quad (8)$$

$$L_j = \frac{k_\perp v_z}{\omega}\left[\frac{\partial f_{0j}}{\partial v_\perp}\cdot\frac{n\omega_{cj}}{k_\perp v_\perp} + \frac{1}{\omega_{cj}}\cdot\frac{\partial f_{0j}}{\partial x}\right] + \left(1 - \frac{n\omega_{cj}}{\omega}\right)\frac{\partial f_{0j}}{\partial v_z}. \quad (9)$$

In the absence of shear flow, Eq. (7) matches exactly with that in the study by Hasegawa.[48] Here, the term $\left(\frac{1}{\omega_{cj}}\cdot\frac{\partial f_{0j}}{\partial x}\right)$ in Eqs. (8) and (9) arises because of the presence of the velocity shear. Equation (8) completely matches with Eq. (7) in the study by Lakhina;[26] however, the Eq. (9) term differs from Eq. (8) in his paper on two counts: one we have $k_\perp$ outside the square bracket instead of $k_\parallel$

which was a typo in his paper and second the term in the parentheses differs by a change of sign [i.e., $\left(1+\frac{n\omega_{cj}}{\omega}\right)$ in his paper]. This arises because of the different forms of perturbation assumed in this paper. Here, $\mathbf{J}_n(\xi_j)$ and $\mathbf{J}_m(\xi_j)$ are the Bessel functions of the order n and m, respectively, with the argument $\xi_j = (k_\perp v_\perp/\omega_{cj})$. We follow the cylindrical coordinates, i.e., $\mathbf{v} = (v_\perp, \theta, v_\parallel)$, where θ represents the angular coordinate of the velocity vector.

Substituting f_{1j} from Eq. (7) into Eq. (5) and performing the velocity integrals, we obtain the following expression for the perturbed number density n_j:

$$
\begin{aligned}
n_j = \frac{e_j}{m_j} N_j \frac{2}{k_\parallel \alpha_j^3} \sum_{n=-\infty}^{+\infty} \mathbf{I}_n(\lambda_j)\exp(-\lambda_j) &\left[\left\{-n\omega_{cj}\left[Z(\mu_j) - \frac{k_\parallel}{\omega} V_j Z(\mu_j)\right]\right.\right. \\
&+ k_\perp S_j\left[\frac{-\alpha_j}{2}Z'(\mu_j) + \frac{k_\parallel}{\omega}\alpha_j^2\left(\frac{\mu_j}{2}+\frac{V_j}{2\alpha_j}\right)Z'(\mu_j)\right]\Big\}\phi \\
&+ \left\{\left(\frac{-n\omega_{cj}}{\omega}k_\parallel\right)\left[-\alpha_j\left\{\frac{1}{2}Z'(\mu_j)-\frac{V_j}{\alpha_j}Z(\mu_j)\right\}\right]\right. \\
&+ \left(\frac{k_\parallel k_\perp}{\omega}S_j\right)\left[-\alpha_j^2\left\{\left(\frac{\mu_j}{2}+\frac{V_j}{2\alpha_j}\right)Z'(\mu_j)\right\}\right] \\
&\left.\left.+ k_\parallel\left(1-\frac{n\omega_{cj}}{\omega}\right)\left[\frac{\alpha_j}{2}Z'(\mu_j)\right]\right\}\psi\right],
\end{aligned}
$$
(10)

and the parallel component (z-component) of the current density J_{zj} as

$$
\begin{aligned}
\mathbf{J}_{zj} = \frac{e_j^2}{m_j} N_j \frac{2}{k_\parallel \alpha_j^3} \sum_{n=-\infty}^{+\infty} &\mathbf{I}_n(\lambda_j) \\
\times \exp(-\lambda_j)&\left[\left\{(-n\omega_{cj})\left[-\alpha_j\left\{\frac{1}{2}Z'(\mu_j)-\frac{V_j}{\alpha_j}Z(\mu_j)\right\}\right.\right.\right. \\
&\left.+ \frac{k_\parallel}{\omega}\alpha_j^2\left\{\frac{V_j}{2\alpha_j}Z'(\mu_j)-\frac{V_j^2}{\alpha_j^2}Z(\mu_j)\right\}\right] \\
&+ k_\perp S_j\left[-\alpha_j^2\left\{\left(\frac{\mu_j}{2}+\frac{V_j}{2\alpha_j}\right)Z'(\mu_j)\right\}\right. \\
&\left.\left.+ \frac{k_\parallel}{\omega}\alpha_j^3\left\{\left(\frac{\mu_j^2}{2}+\frac{V_j}{\alpha_j}\mu_j+\frac{1}{2}\frac{V_j^2}{\alpha_j^2}\right)Z'(\mu_j)-\frac{1}{2}\right\}\right]\right\}\phi \\
&+ \left\{\left(\frac{-n\omega_{cj}}{\omega}k_\parallel\right)\left[-\alpha_j^2\left\{\left(\frac{\mu_j}{2}+\frac{V_j}{\alpha_j}\right)Z'(\mu_j)-\frac{V_j^2}{\alpha_j^2}Z(\mu_j)\right\}\right]\right. \\
&+ \left(\frac{k_\parallel k_\perp}{\omega}S_j\right)\left[-\alpha_j^3\left\{\left(\frac{\mu_j^2}{2}+\frac{V_j}{\alpha_j}\mu_j+\frac{1}{2}\frac{V_j^2}{\alpha_j^2}\right)Z'(\mu_j)-\frac{1}{2}\right\}\right] \\
&\left.\left.+ \left[-k_\parallel\left(1-\frac{n\omega_{cj}}{\omega}\right)\right]\left[-\alpha_j^2\left\{\left(\frac{\mu_j}{2}+\frac{V_j}{2\alpha_j}\right)Z'(\mu_j)\right\}\right]\right\}\psi\right],
\end{aligned}
$$
(11)

where $Z(\mu_j)$ is the plasma dispersion function, $Z'(\mu_j)$ is the derivative of the plasma dispersion function with respect to its argument $\mu_j = \frac{\omega - k_\parallel V_j}{k_\parallel \alpha_j}$, $\mathbf{I}_n(\lambda_j)$ is the modified Bessel function of order n with the argument $\lambda_j = \left(\frac{k_\perp^2 \alpha_j^2}{2\omega_{cj}^2}\right)$, and $S_j = \left(\frac{1}{\omega_{cj}}\right)\cdot\frac{dV_j}{dx}$ represents the velocity shear.

Substituting perturbed number density from Eq. (10) and current density from Eq. (11) into Eqs. (3) and (4), respectively, and assuming low frequency waves ($\omega^2 \ll \omega_{cj}^2$) propagating nearly perpendicular to $\mathbf{B}_0$, i.e., $k_\parallel^2 \ll k_\perp^2$, we obtain the following:

$$D_{11}\phi + D_{12}\psi = 0,$$
(12)
$$D_{21}\phi + D_{22}\psi = 0,$$
(13)

where

$$D_{11} = k_\perp^2\left[1+\sum_j \frac{2\omega_{pj}^2}{k_\perp^2 \alpha_j^2}\frac{\bar{\omega}}{\omega}(1-b_j)\right],$$
(14)

$$D_{12} = k_\parallel^2\left[1-\sum_j \frac{\omega_{pj}^2 b_j}{k_\parallel^2 \alpha_j^2}Z'\left(\frac{\bar{\omega}}{k_\parallel \alpha_j}\right)\left(1-S_j\frac{k_\perp}{k_\parallel}\right)\right],$$
(15)

$$D_{21} = k_\parallel k_\perp^2\left[1+\sum_j \frac{\omega_{pj}^2 b_j}{c^2 k_\perp^2}S_j\frac{k_\perp}{k_\parallel}\right],$$
(16)

$$D_{22} = -k_\parallel k_\perp^2\left[1+\sum_j \frac{\omega_{pj}^2}{c^2 k_\perp^2}\left\{\frac{b_j \omega^2}{k_\parallel^2 \alpha_j^2}Z'\left(\frac{\bar{\omega}}{k_\parallel \alpha_j}\right)\left(1-S_j\frac{k_\perp}{k_\parallel}\right)+S_j\frac{k_\perp}{k_\parallel}\right\}\right],$$
(17)

where $\omega_{pj} = \left(\frac{4\pi N_j e_j^2}{m_j}\right)^{1/2}$ is the plasma frequency, $\bar{\omega} = (\omega - k_\parallel V_j)$ the Doppler shifted frequency of jth species; $b_j = \mathbf{I}_0(\lambda_j)\exp(-\lambda_j)$, where $\mathbf{I}_0(\lambda_j)$ is the modified Bessel function of order zero. These expressions match quite well with those in the study by Lakhina[26] except that k^2 is replaced by $k_\perp^2$ in the second term within the square bracket of D_{11} which was a typo in that paper. It is pointed out here that while deriving D_{11}, D_{12}, D_{21}, and D_{22} components, the modified Bessel function for the electron terms has been expanded in the limit $\lambda_e \ll 1$ and leading order terms have been retained. It must be emphasized here that though the expressions appearing in this paper have been derived earlier by Lakhina,[26] we are writing these here because some typos were found in some of the expressions.

The dispersion relation is obtained from Eqs. (12) and (13) by equating the determinant of the coefficients of ϕ and ψ to zero, which is expressed as

$$
\begin{aligned}
1 + &\sum_j \frac{\omega_{pj}^2}{k^2 \alpha_j^2}\left[\frac{2\bar{\omega}}{\omega}(1-b_j)-b_j\left(1-S_j\frac{k_\perp}{k_\parallel}\right)Z'\left(\frac{\bar{\omega}}{k_\parallel \alpha_j}\right)\right] \\
&+ \sum_j \frac{2\omega_{pj}^2}{k^2 \alpha_j^2}\frac{\bar{\omega}}{\omega}(1-b_j)\cdot\sum_j \frac{\omega_{pj}^2}{c^2 k_\perp^2}\left[\frac{b_j \omega^2}{k_\parallel^2 \alpha_j^2}Z'\left(\frac{\bar{\omega}}{k_\parallel \alpha_j}\right)\left(1-S_j\frac{k_\perp}{k_\parallel}\right)+S_j\frac{k_\perp}{k_\parallel}\right] \\
&- \sum_j \frac{\omega_{pj}^2 b_j}{k^2 \alpha_j^2}\left(1-S_j\frac{k_\perp}{k_\parallel}\right)Z'\left(\frac{\bar{\omega}}{k_\parallel \alpha_j}\right)\cdot\sum_j \frac{\omega_{pj}^2 b_j}{c^2 k_\perp^2}S_j\frac{k_\perp}{k_\parallel}=0.
\end{aligned}
$$
(18)

This generalized dispersion relation Eq. (18) is exactly the same as in the study by Lakhina[26] in which k^2 is replaced by $k_\perp^2$ in the second summation of the last term.

III. DISPERSION RELATION: HOT ION BEAM CASE

Here, we proceed in the same manner as Lakhina[26] and obtain a dispersion relation by considering the hot ion beam case. To start with, we assume that the background ions and

electrons have no drift velocity and shear flow, i.e., $V_i = V_e = 0, S_i = S_e = 0$. Furthermore, we assume the hot ion beam with a drift velocity V_B and shear in the flow as $S = S_B$. The following assumptions are in order: for the hot ion beam which is the source of free energy, $\bar{\omega} \ll k_\parallel \alpha_B$, for hot electrons, $\omega \ll k_\parallel \alpha_e, \lambda_e \ll 1$, and for the cold and stationary background ions, $\omega^2 \gg k_\parallel^2 \alpha_i^2$. With the assumptions discussed above, we obtain the following simplified dispersion relation from Eq. (18):

$$\frac{b_i N_i}{N_e}\left[1 + a_1 - \frac{\omega^2}{k_\parallel^2 v_A^2}\frac{N_i}{N_e}\frac{1-b_i}{\lambda_i}Aq_0\right]$$
$$-\frac{\omega^2}{k_\parallel^2 c_s^2}\left[C_R' + i(1+a_1)C_I - \frac{\omega^2}{k_\parallel^2 v_A^2}\frac{N_i}{N_e}\frac{1-b_i}{\lambda_i}A(C_R + iC_I)\right]$$
$$= \frac{2\omega^2}{k_\parallel^2 \alpha_i^2}\frac{(1-b_i)N_i}{N_e}, \qquad (19)$$

where

$$a_1 = \frac{N_B}{N_e}\frac{\beta_B b_B}{2\lambda_B}S\frac{k_\perp}{k_\parallel}, \qquad (20)$$

$$q_0 = 1 + \frac{N_B}{N_i}\frac{m_i}{m_B}\frac{Sk_\perp}{b_i k_\parallel}, \qquad (21)$$

$$A = 1 + \frac{N_B}{N_i}\frac{T_i}{T_B}\frac{\bar{\omega}}{\omega}\frac{(1-b_B)}{(1-b_i)}, \qquad (22)$$

$$C_R = 1 + \frac{N_B}{N_e}\frac{T_e}{T_B}b_B\left(1 - S\frac{k_\perp}{k_\parallel}\right), \qquad (23)$$

$$C_R' = 1 + \frac{N_B}{N_e}\frac{T_e}{T_B}\left\{b_B\left(1 - \frac{\bar{\omega}}{\omega}\right) + \left(\frac{\bar{\omega}}{\omega} - b_B S\frac{k_\perp}{k_\parallel}\right)\right\} + a_1 C_R, \qquad (24)$$

$$C_I = \sqrt{\pi}\frac{\omega}{k_\parallel \alpha_e}\left[\exp\left(-\frac{\omega^2}{k_\parallel^2 \alpha_e^2}\right) + b_B\frac{N_B}{N_e}\left(\frac{T_e}{T_B}\right)^{3/2}\right.$$
$$\left.\times\left(\frac{m_B}{m_e}\right)^{1/2}\frac{\bar{\omega}}{\omega}\left(1 - S\frac{k_\perp}{k_\parallel}\right)\exp\left(-\frac{\bar{\omega}^2}{k_\parallel^2 \alpha_B^2}\right)\right]. \qquad (25)$$

Here, all the above expressions match perfectly well with those in the study by Lakhina[26] except the term a_1 which has the extra factor of $(k_\perp^2/k^2)$ in that paper, which was due to the discrepancy in Eq. (18) as mentioned earlier. In the above expression, C_I represents the damping arising due to hot electrons and beam ions, and $c_s = (T_e/m_i)^{1/2}$ is the ion acoustic speed, $v_A = (B_0^2/4\pi N_e m_i)^{1/2}$ is the Alfvén velocity, and $\beta_i = (8\pi N_e T_i/B_0^2)$ and $\beta_B = (8\pi N_e T_B/B_0^2)$ are ion and beam plasma betas, respectively.

It must be mentioned here that in the absence of the ion-beam ($N_B = 0$) in Eq. (19) and neglecting the damping due to

electrons and the ion beam, we obtain the usual dispersion relation for KAWs in two-components, i.e., electron-proton plasma as shown by Eq. (36) in the study by Hasegawa and Chen[18] and Eq. (23) in the study by Lakhina.[26] The general dispersion relation Eq. (19) can now be written as

$$D_R(\omega, k) + iD_I(\omega, k) = 0, \qquad (26)$$

where

$$D_R(\omega, k) = \frac{\omega^4}{k_\parallel^4 V_A^4}\left[\frac{N_i}{N_e}\frac{(1-b_i)}{\lambda_i}AC_R\right] - g_1\frac{\omega^2}{k_\parallel^2 V_A^2} + \frac{N_i}{N_e}\frac{b_i \beta_i}{2}\frac{T_e}{T_i}(1+a_1), \qquad (27)$$

$$D_I(\omega, k) = -\frac{\omega^2}{k_\parallel^2 V_A^2}\left[1 + a_1 - \frac{\omega^2}{k_\parallel^2 V_A^2}\frac{(1-b_i)}{\lambda_i}\frac{N_i}{N_e}A\right]C_I, \qquad (28)$$

$$g_1 = \left[C_R' + \frac{N_i}{N_e}(1-b_i)\frac{T_e}{T_i}\left\{1 + \frac{N_i}{N_e}\frac{b_i \beta_i}{2\lambda_i}Aq_0\right\}\right], \qquad (29)$$

$$g_0 = \left(\frac{N_i}{N_e}\right)^2\frac{b_i \beta_i}{2}\frac{T_e}{T_i}\frac{(1-b_i)}{\lambda_i}(1+a_1)AC_R. \qquad (30)$$

The real frequency can be obtained by equating $D_R(\omega, k) = 0$ and hence is given by

$$\frac{\omega^4}{k_\parallel^4 V_A^4}\left[\frac{N_i}{N_e}\frac{(1-b_i)}{\lambda_i}AC_R\right] - g_1\frac{\omega^2}{k_\parallel^2 V_A^2} + \frac{N_i}{N_e}\frac{b_i \beta_i}{2}\frac{T_e}{T_i}(1+a_1) = 0, \quad (31)$$

which contains both shear and beam velocity. Analytically, it is quite difficult to solve Eq. (31) as the coefficients A, C_R' and g_1 contain $\bar{\omega} = \omega - k_\parallel V_B$ terms. Expression (31) in the study by Lakhina[26] can be obtained in the absence of streaming $V_B = 0$ and $C_I \approx 0$. The threshold condition for excitation of non-resonant instabilities is obtained with $C_R < 0$ and is given by

$$S_{th} = \frac{k_\parallel}{k_\perp}\left[1 + \frac{N_e}{N_B}\frac{T_B}{T_e b_B}\right]. \qquad (32)$$

Lakhina[26] has carried out the analysis for non-resonant and resonant instabilities excited by the ion shear flow only. The purpose of the present paper is to study the effect of the ion beam and ion shear flow on the resonant instability. We also study the combined effect of ion beam velocity and ion shear flow on the instability.

A. Resonant instability

The growth/damping rate of KAWs can be obtained from Eq. (26) by assuming $\omega = \omega_r + i\gamma$, where ω_r is the real frequency and $\gamma \ll \omega_r$ is the growth/damping rate of the wave. The growth/damping rate of the resonant instability is given by

$$\gamma = -\frac{D_I(\omega_r, \mathbf{k})}{\dfrac{\partial D_R(\omega_r, \mathbf{k})}{\partial \omega_r}} = \frac{\omega_r^2\left[1 + a_1 - \dfrac{\omega_r^2}{k_\parallel^2 v_A^2}\dfrac{(1-b_i)}{\lambda_i}\dfrac{N_i}{N_e}A\right]C_I}{\omega_r\left\{2(g_1^2 - 4g_0)^{1/2}\right\} + k_\parallel V_B\dfrac{N_B}{N_e}(1-b_B)\left\{\dfrac{\omega_r^2}{k_\parallel^2 v_A^2}\dfrac{T_i}{T_B}\dfrac{C_R}{\lambda_i} - \dfrac{T_e}{T_B}\left[1 + \dfrac{N_i}{N_e}\dfrac{b_i \beta_i}{2\lambda_i}q_0\right]\right\}}. \qquad (33)$$

This is a general expression for the growth/damping rate of KAWs. In the absence of ion streaming ($V_B = 0$), we can retrieve Eq. (31) in the study by Lakhina.[26]

It is worth mentioning here that the dispersion relation (19) is a coupled one between the ion acoustic and the kinetic Alfvén waves. In the limit of low plasma beta, the coupling becomes weak and the two waves decouple. The instability of electrostatic waves may consume some of the free energy of the beam to suppress the growth of the kinetic Alfvén waves. Usually, the electrostatic modes are of shorter wave lengths but have larger growth rates as compared to electromagnetic modes. They are the ones to saturate first, leaving rest of the free energy for the electromagnetic modes to grow. Even if the ion acoustic instability is excited, we believe that it cannot dissipate all the free energy available in the system. There may still be enough free energy available which can lead to the growth of kinetic Alfvén waves. All of our numerical calculations have been carried out in the low plasma beta limit, i.e., $\beta_i \ll 0.01$. Hence, electrostatic ion acoustic waves are excluded and our main focus is to study the resonant instability of KAWs.

The numerical computations are carried out for real frequency [Eq. (31)] and growth/damping rate [Eq. (33)] for the plasma parameters for which all the assumptions made in the theoretical analysis are satisfied. For ease of numerical computations, the dispersion relation is normalized as follows: frequencies, ω_r, are normalized with respect to the cyclotron frequency of the ion beam, ω_{cB}, temperatures with ion beam temperature, T_B, and streaming velocity, V_B, with the thermal speed of the ion beam, α_B. Throughout the manuscript, normalized real frequency and the growth rates of the resonant instability as calculated from Eqs. (31) and (33), respectively, are plotted against $\lambda_B = k_\perp^2 \alpha_B^2 / 2\omega_{cB}^2$ (square of the perpendicular wave number normalized with the gyroradius of the beam ions). Numerical computations show that the resonant instability of the KAW will occur when $C_R > 0$ and $C_I < 0$.

Figures 1(a) and 1(b) show the variation of the normalized real frequency and growth/damping rate of the resonant KAW instability driven by the ion beam versus square of the normalized perpendicular wave number $\lambda_B = \frac{k_\perp^2 \alpha_B^2}{2\omega_{cB}^2}$. The plasma parameters are fractional ion beam density, $\frac{N_B}{N_e} = 0.5$, $\beta_i = 0.001$, $\frac{k_\parallel}{k_\perp} = 0.01$, $S = 0$

and for various values of the ion beam velocity as indicated on the curves itself.

Here, in the absence of velocity shear, the effect of ion beam velocity can be seen on the growth of KAWs. It is observed from the figures that the real frequency as well as the growth rate increases with the increase in ion beam velocity. The increase in real frequency at a fixed wavenumber is marginal, whereas the growth rate increases significantly. It is observed that the peak in the growth rate shifts towards the higher λ_B values with the increase in ion beam velocity. Our numerical computations reveal that for the above given parameters, for the excitation of KAWs, **the threshold value** on the ion beam velocity comes out to be $\frac{V_B}{\alpha_B} \approx 0.4$.

In Fig. 2, we plot the real frequency and growth rate with finite shear ($S = 0.5$) and ion beam streaming opposite to the magnetic field direction with the values mentioned on the curves, keeping other parameters the same as those in Fig. 1. It is observed that with finite velocity shear, when ion beam velocity is increased in the anti-parallel direction to the ambient magnetic field, the real frequency decreases, whereas the growth rate increases. However, it is clear from Fig. 3 that in the presence of finite positive shear ($S = 0.5$), when the ion beam velocity parallel to the ambient magnetic field is increased, the real frequency increases, whereas the growth rate decreases. There is no growth of KAWs beyond $\frac{V_B}{\alpha_B} = 0.2$. Hence, it is concluded that whenever a finite positive shear is present, the antiparallel streaming ion beam favors the excitation of the KAWs, whereas the parallel ion beam has a stabilizing effect.

In Fig. 4, we show the variation of the real frequency and growth rate of the KAWs driven by the finite ion beam in the absence of the velocity shear (i.e., $S = 0$) for various values of ion beam density for $V_B/\alpha_B = 0.9$. Other parameters are the same as in Fig. 1. It is observed that with the increase in ion beam density, the real frequency decreases, whereas the growth rate increases. Furthermore, the peak in the growth rate shifts towards a higher λ_B value. It is interesting to note that the **critical value** of number density is found as $N_B/N_e \approx 0.2$ below which no growth is found. However, when the finite negative velocity shear, $S = -0.2$, is introduced for the parameters of Fig.
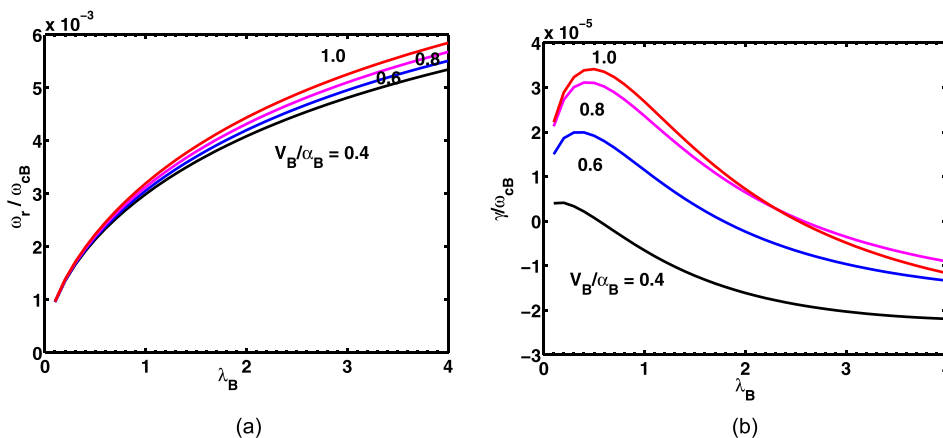

FIG. 1. KAW resonant instability driven by the ion beam: Variation of (a) normalized real frequency, ω_r/ω_{cB}, and (b) normalized growth rate, γ/ω_{cB} versus $\lambda_B = \frac{k_\perp^2 \alpha_B^2}{2\omega_{cB}^2}$ for $\frac{N_B}{N_e} = 0.5$, $\beta_i = 0.001$, $\frac{k_\parallel}{k_\perp} = 0.01$, $S = 0$ and various values of $\frac{V_B}{\alpha_B}$ as listed on the curves.
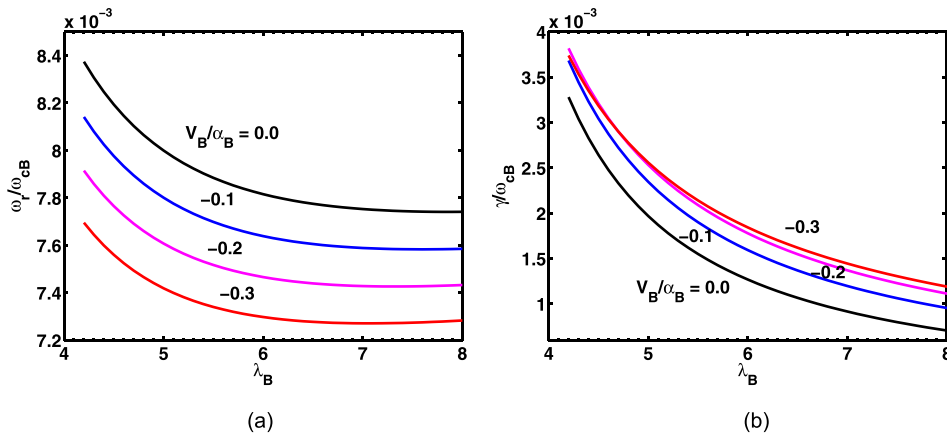
FIG. 2. KAW resonant instability driven by ion beam streaming in a direction opposite to the magnetic field and positive velocity shear (a) Normalized real frequency and (b) normalized growth rate versus λ_B for $S = 0.5$ and various values of $\frac{V_B}{\alpha_B}$ as listed on the curves. All other parameters are as in Fig. 1.
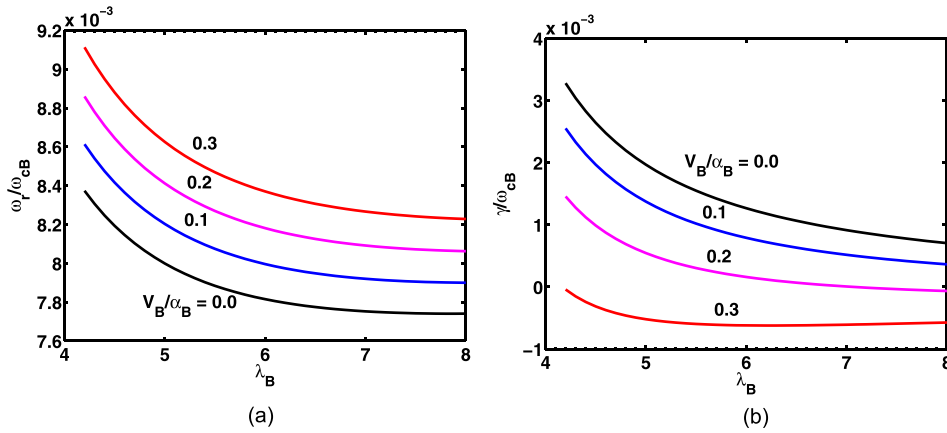

FIG. 3. KAW resonant instability driven by the parallel streaming ion beam and positive velocity shear: (a) normalized real frequency and (b) normalized growth rate versus λ_B for $\frac{N_B}{N_e} = 0.5$, $\beta_i = 0.001$, $\frac{k_\parallel}{k_\perp} = 0.01$, $S = 0.5$. and various values of $\frac{V_B}{\alpha_B}$ as listed on the curves.

4, the behaviour of the real frequency and growth rate remains the same as in Fig. 4 but the **critical value** of the beam density lowers to **0.1** (not shown).

In Figs. 5 and 6, the variation of the real frequency and growth rate is shown with $k_\parallel/k_\perp$ in the absence and presence of velocity shear, respectively. It is observed that in both the cases,

the real frequency and the growth rate increase with the increase in $k_\parallel/k_\perp$ values. The growth rate is more in the presence of negative shear and ion beam as compared to the case of the ion beam alone.

In Figs. 7 and 8, the effect of $\frac{T_e}{T_B}$ is examined without velocity shear ($S = 0$) and with negative velocity shear ($S = -0.2$),
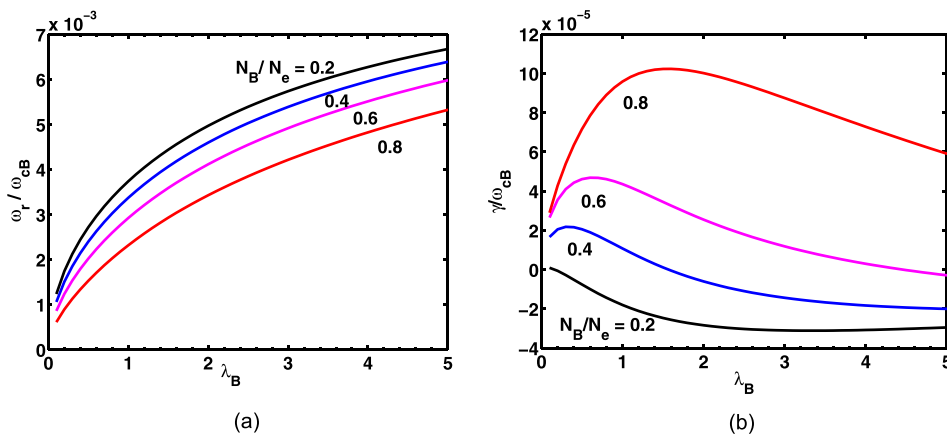

FIG. 4. Resonant instability of KAWs driven by the ion beam: (a) normalized real frequency and (b) normalized growth rate versus λ_B for $\beta_i = 0.001$, $\frac{k_\parallel}{k_\perp} = 0.01$, $S = 0.0$, $\frac{V_B}{\alpha_B} = 0.9$ and various values of $\frac{N_B}{N_e}$ as listed on the curves.
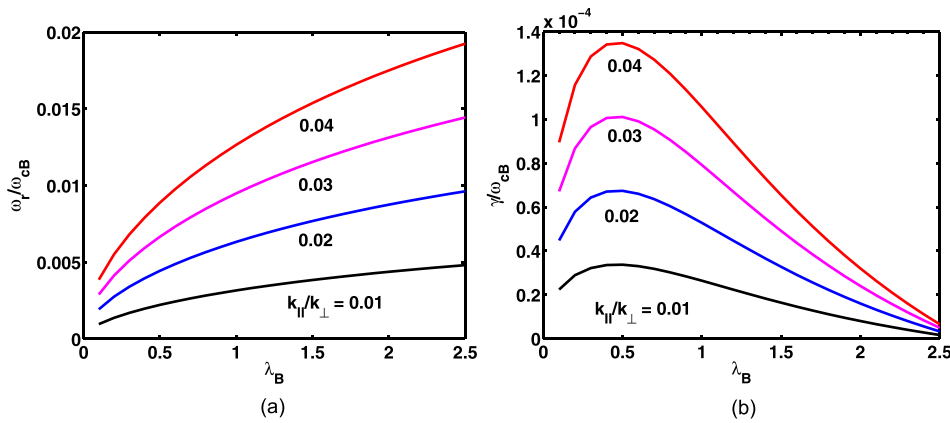
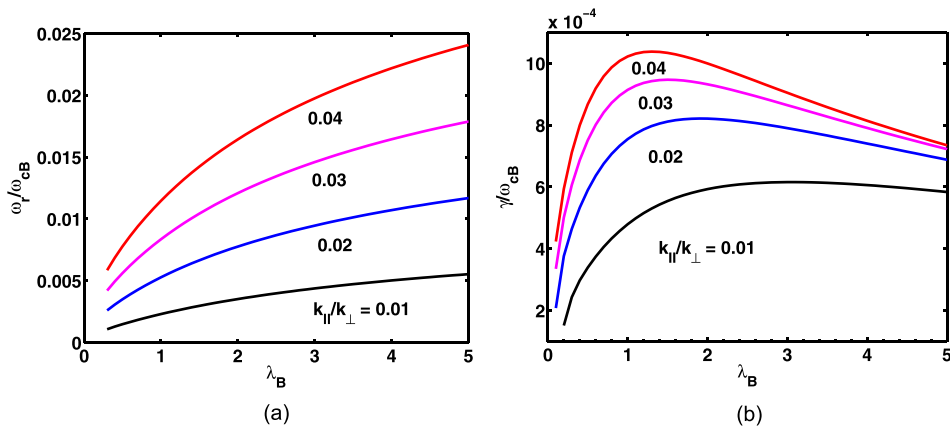**FIG. 5.** Resonant instability of KAWs driven by the ion beam: (a) normalized real frequency and (b) normalized growth rate versus λ_B for $\frac{N_B}{N_e} = 0.5$, $\beta_i = 0.001$, S= 0, $\frac{V_B}{\alpha_B} = 0.9$ and various values of $\frac{k_\parallel}{k_\perp}$ as listed on the curves.

FIG. 6. Resonant instability of KAWs driven by the ion beam and negative velocity shear: (a) normalized real frequency and (b) normalized growth rate versus λ_B for $\frac{N_B}{N_e} = 0.5$, $\beta_i = 0.001$, S $= -0.2$, $\frac{V_B}{\alpha_B} = 0.9$ and various values of $\frac{k_\parallel}{k_\perp}$ as listed on the curves.

respectively, in the presence of finite ion beam velocity. In both the cases, the growth rate as well as the real frequency increases with the increase in $\frac{T_e}{T_B}$ values. The growth rate peaks are sharper in Fig. 7, whereas they are broader in Fig. 8, and in both the cases, growth rate peaks shift towards the higher λ_B values. The growth rate is significantly higher in the case where negative shear and ion beams are present as compared to the without velocity

shear case. Though not presented here, numerical results show that the effects of $\frac{T_i}{T_B}$ and β_i on the growth of instability are negligible for the plasma parameters considered here.

IV. DISCUSSION AND CONCLUSIONS

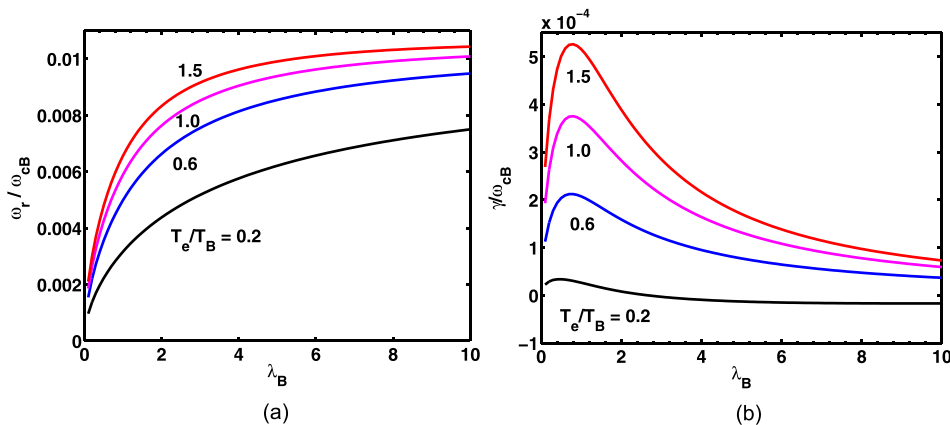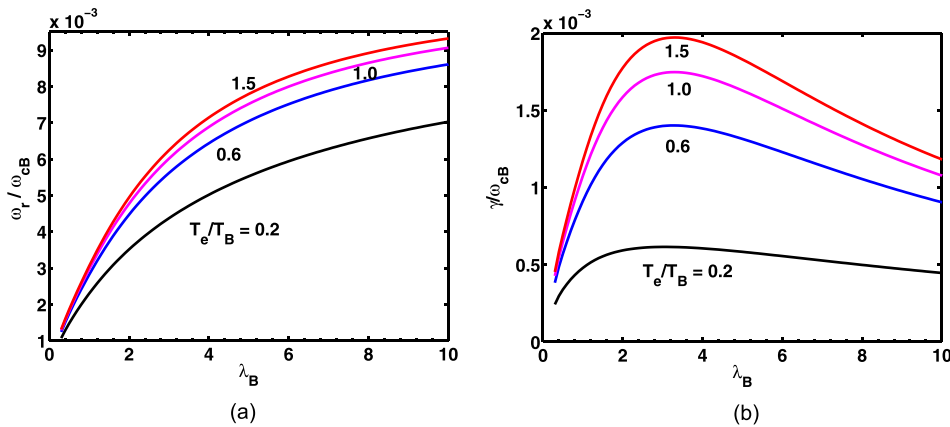Kinetic Alfvén waves have been studied in a three-component plasma consisting of the background cold ions, hot

FIG. 7. Resonant instability of KAWs driven by the ion beam: (a) normalized real frequency and (b) normalized growth rate versus λ_B for $\frac{N_B}{N_e} = 0.5$, $\beta_i = 0.001$, S= 0, $\frac{V_B}{\alpha_B} = 0.9$, $\frac{k_\parallel}{k_\perp} = 0.01$ and various values of $\frac{T_e}{T_B}$ as listed on the curves.

FIG. 8. Resonant instability of KAWs driven by the ion beam and negative velocity shear: (a) normalized real frequency and (b) normalized growth rate versus λ_B for $\frac{N_B}{N_e} = 0.5$, $\beta_i = 0.001$, $S = -0.2$, $\frac{V_B}{\alpha_B} = 0.9$, $\frac{k_\parallel}{k_\perp} = 0.01$ and various values of $\frac{T_e}{T_B}$ as listed on the curves.

electrons, and hot ion beams. These waves are driven by ion beams as well as shear in the ion beam velocity. The main focus of this paper is to study the ion beam as well as velocity shear driven resonant instability of kinetic Alfvén waves. Therefore, in this model, a comparison of results obtained with only ion beam (no shear) and with ion beams with velocity shear is made. It is found that the ion beam alone can drive KAWs with a significant growth rate. It is observed that when positive velocity shear is present and the ion beam is streaming parallel to the ambient magnetic field, the growth rate of KAWs significantly reduces and it has a stabilizing effect. On the other hand, for the ion beam streaming anti-parallel to the ambient magnetic field but having positive velocity shear, there is a marked increase in the growth rate of KAWs.

In the literature, the physical mechanism for the electrostatic instabilities is ascribed to the bunching of the charges,[49–51] and for the electromagnetic instabilities, it is attributed to bunching of the current[52–55] and Landau resonance.[56] The electromagnetic instabilities arise when the Lorentz force due to the fluctuating magnetic field causes momentum fluxes and bunching of currents at some locations leading to enhancement of the initial magnetic perturbation. We are not aware of any physical mechanism for the kinetic Alfvén instability, but expect the current bunching as a physical cause irrespective of the nature of the free energy source, i.e., whether it is temperature anisotropy, beam, or the velocity shear. In our case, when the ion beams propagate anti-parallel to ambient magnetic field B_0, the velocity shear seems to increase (disperse) the current bunching when it is along the positive (negative) x-axis. The role of velocity shear is reversed when the ion beam is propagating along B_0.

For an application of our model, we consider some typical plasma parameters observed on the auroral/polar cusp field lines at an altitude of 5–7 R_E, where R_E is the radius of the Earth.[2,3,26] The reported hot ion beam densities and speed are $N_B/N_e = (0.01 - 0.2)$, beam speed, $V_B/\alpha_B < 2$, respectively. For our numerical computations, we assume $N_B/N_e = (0.1–0.8)$, $V_B/\alpha_B = (-1.2$ to $1.2)$, $\beta_i = (0.001–0.01)$, and $S = (-0.2$ to $0.5)$. We also consider $\frac{\omega_{cB}}{2\pi} \approx (2.2 - 3)$ Hz which is common at the auroral altitude of 5–7 R_E, the hot electron temperature, $T_e \approx 100$ eV, the background cold ion temperature, $T_i \approx 10$ eV, and the ion beam

temperature, $T_B \approx 1$–2 keV. From our assumption of local approximation, we obtain $\lambda_B \gg \lambda_B^* = (S\alpha_B/V_B)^2 = (0.1736 -1.5625)$ for $S = 0.5$ and $V_B/\alpha_B = (0.4–1.2)$, whereas $\lambda_B^* = 0$ for the case of pure ion beam velocity, i.e., when velocity shear is zero. For all these above values, the graphs are plotted and the results are shown in the respective figures.

The maximum normalized growth rate (γ/ω_{cB}) and the corresponding normalized real frequency (ω_r/ω_{cB}) for resonant instability driven by the ion beam alone (Fig. 5, $S = 0.0$, $V_B/\alpha_B = 0.9$, $k_\parallel/k_\perp = 0.04$) are found to be 0.00014 and 0.009 at $\lambda_B = 0.5$ and are excited for $\lambda_B = 0.1$–2.5. Then, the unnormalized growth rate and the real frequency are 0.00035 Hz and 0.0225 Hz, respectively, for $\frac{\omega_{cB}}{2\pi} = 2.5$ Hz. The real frequency value for the whole range of our computation falls in the range of $\approx (10$–50) mHz for the above-mentioned case. The growth rate is in the range of (0.02–0.35) mHz. The corresponding transverse wave number which can be calculated from the relation $k_\perp = (\lambda_B^{1/2}/\rho_B)$, where $\rho_B = (\alpha_B/2^{1/2}\omega_{cB})$ is the gyro-radius of the ion beams, is found to be in the range $k_\perp \approx (0.01$–0.06) km^{-1}. The respective perpendicular wavelength lies in the range of (628–105) km. The corresponding parallel wave number can be obtained from the relation $k_\parallel/k_\perp = 0.04$ and is found to be $k_\parallel \approx (0.04$–0.24) $\times 10^{-2}$ km^{-1} and the parallel wavelength $\approx (157$–26) $\times 10^2$ km. On the other hand, in the presence of both the ion beam velocity and velocity shear (Fig. 6, $S = -0.2$, $V_B/\alpha_B = 0.9$, $k_\parallel/k_\perp = 0.04$), the maximum value of the normalized real frequency and growth rate for resonant instability is found to be 0.013 and 0.001, respectively, at $\lambda_B = 1.3$ and is excited in the range of $\lambda_B = (0.3$–5.0). The real frequency has a value of $\approx (15$–60) mHz for the full range of computation. The corresponding growth rate is in the range of (1–2.5) mHz. The ULF waves with a frequency of 0.0325 Hz can be excited with a significant growth rate of 0.0025 Hz for $\frac{\omega_{cB}}{2\pi} = 2.5$ Hz. The perpendicular wave number calculated as earlier falls in the range of $k_\perp \approx (0.02$–0.08) km^{-1} and the corresponding wavelength is in the range of (314–78) km. The parallel wave number is found as $k_\parallel \approx (0.08$–0.32) $\times 10^{-2}$ km^{-1} and the corresponding parallel wavelength is obtained as (78–20) $\times 10^2$ km. Furthermore, in the presence of both the ion beam and velocity shear, KAWs with much larger growth rates are excited as compared to the case

of the ion beam alone. It is also observed that KAWs have a larger growth rate with positive velocity shear and an anti-parallel ion beam as compared to negative velocity shear and a parallel ion beam.

It is emphasized here that our theoretical model can excite the ULF waves where ion beams or velocity shear exists. Also, for the first time, we have shown the combined effect of ion beam and velocity shear on the generation of KAWs. In both the cases, i.e., ion beam alone as well as combined ion beam and velocity shear, the KAWs with a range of frequencies $\approx$(10–60) mHz can be excited. The predicted perpendicular wavelengths of (78–628) km compare fairly well with the Polar observations[10] of the perpendicular scale size of (20–120) km. The predicted ULF wave frequencies and wavelengths from our model may be relevant in understanding the properties of the low-frequency electromagnetic waves observed in the Earth's magnetosphere.

ACKNOWLEDGMENTS

REFERENCES

[1]N. D'Angelo, J. Geophys. Res. **78**, 1206, https://doi.org/10.1029/JA078i007p01206 (1973).

[2]N. D'Angelo, A. Bahnsen, and H. Rosenbauer, J. Geophys. Res. **79**, 3129, https://doi.org/10.1029/JA079i022p03129 (1974).

[3]D. A. Gurnett and L. A. Frank, J. Geophys. Res.: Space Phys. **83**, 1447, https://doi.org/10.1029/JA083iA04p01447 (1978).

[4]S. A. Curtis, W. R. Hoegy, L. H. Brace, N. C. Maynard, M. Suguira, and J. D. Winningham, Geophys. Res. Lett. **9**, 997, https://doi.org/10.1029/GL009i009p00997 (1982).

[5]P. Song, C. T. Russell, R. J. Strangeway, J. R. Wygant, C. A. Cattell, R. J. Fitzenreiter, and R. R. Anderson, J. Geophys. Res. **98**, 187, https://doi.org/10.1029/92JA01534 (1993).

[6]L. Rezeau, A. Morane, S. Perraut, A. Roux, and R. Schmidt, J. Geophys. Res. **94**, 101–110, https://doi.org/10.1029/JA094iA01p00101 (1989).

[7]L. Rezeau, A. Roux, and C. T. Russell, J. Geophys. Res. **98**, 179, https://doi.org/10.1029/92JA01668 (1993).

[8]B. J. Anderson and M. J. Engebretson, J. Geophys. Res. **100**, 9591, https://doi.org/10.1029/95JA00132 (1995).

[9]J. R. Johnson and C. Z. Cheng, Geophys. Res. Lett. **24**, 1423–1426, https://doi.org/10.1029/97GL01333 (1997).

[10]J. R. Wygant, A. Keiling, C. A. Cattell, R. L. Lysak, M. Temerin, F. S. Mozer, C. A. Kletzing, J. D. Scudder, V. Streltsov, W. Lotko, and C. T. Russell, J. Geophys. Res.: Space Phys. **107**, SMP 24, https://doi.org/10.1029/2001ja900113 (2002).

[11]K. Nykyri, P. J. Cargill, E. A. Lucek, T. S. Horbury, A. Balogh, B. Lavraud, I. Dandouras, and H. Rème, Geophys. Res. Lett. **30**, SSC-12, https://doi.org/10.1029/2003GL018594 (2003).

[12]D. Sundkvist, A. Vaivads, M. André, J.-E. Wahlund, Y. Hobara, S. Joko, V. Krasnoselskikh, Y. Bogdanova, S. Buchert, N. Cornilleau-Wehrlin et al., Ann. Geophys. **23**, 983 (2005).

[13]T. Takada, K. Seki, M. Hirahara, M. Fujimoto, Y. Saito, H. Hayakawa, and T. Mukai, J. Geophys. Res.: Space Phys. **110**, A02204, https://doi.org/10.1029/2004JA010395 (2005).

[14]B. Grison, F. Sahraoui, B. Lavraud, T. Chust, N. Cornilleau-Wehrlin, H. Reme, A. Balogh, and M. André, Ann. Geophys. **23**, 3699 (2005).

[15]N. D'Angelo, Rev. Geophys. **15**, 299, https://doi.org/10.1029/RG015i003p00299 (1977).

[16]L. Chen and A. Hasegawa, J. Geophys. Res. **79**, 1024, https://doi.org/10.1029/JA079i007p01024 (1974).

[17]J. D. Huba, J. Geophys. Res.: Space Phys. **86**, 8991, https://doi.org/10.1029/JA086iA11p08991 (1981).

[18]A. Hasegawa and L. Chen, Phys. Fluids **19**, 1924 (1976).

[19]C. K. Goertz and R. W. Boswell, J. Geophys. Res. **84**, 7239, https://doi.org/10.1029/JA084iA12p07239 (1979).

[20]R. L. Lysak and C. T. Dum, J. Geophys. Res. **88**, 365, https://doi.org/10.1029/JA088iA01p00365 (1983).

[21]G. S. Lakhina, J. Geophys. Res.: Space Phys. **92**, 12161, https://doi.org/10.1029/JA092iA11p12161 (1987).

[22]G. S. Lakhina, Astrophys. Space Sci. **165**, 153 (1990).

[23]R. L. Lysak and W. Lotko, J. Geophys. Res.: Space Phys. **101**, 5085, https://doi.org/10.1029/95JA03712 (1996).

[24]B. J. Thompson and R. L. Lysak, J. Geophys. Res.: Space Phys. **101**, 5359, https://doi.org/10.1029/95JA03622 (1996).

[25]M. Nose, T. Iyemori, M. Sugiura, J. A. Slavin, R. A. Holfman, J. D. Winningham, and N. Sato, J. Geophys. Res. **103**, 17587, https://doi.org/10.1029/98JA01187 (1998).

[26]G. S. Lakhina, Adv. Space Res. **41**, 1688 (2008).

[27]M. Temerin, J. McFadden, M. Boehm, C. W. Carlson, and W. Lotko, J. Geophys. Res.: Space Phys. **91**, 5769, https://doi.org/10.1029/JA091iA05p05769 (1986).

[28]T. K. Nakamura, J. Geophys. Res. **105**, 10729, https://doi.org/10.1029/1999JA900494 (2000).

[29]J. R. Johnson, C. Z. Cheng, and P. Song, Geophys. Res. Lett. **28**(2), 227–230, https://doi.org/10.1029/2000GL012048 (2001).

[30]C. C. Chaston, L. M. Peticolas, C. W. Carlson, J. P. McFadden, F. Mozer, M. Wilber, G. K. Parks, A. Hull, R. E. Ergun, R. J. Strangeway et al., J. Geophys. Res.: Space Phys. **110**, A02211, https://doi.org/10.1029/2004JA010483 (2005).

[31]D. J. Gershman, A. F. Vias, J. C. Dorelli, S. A. Boardsen, L. A. Avanov, P. M. Bellan, S. J. Schwartz, B. Lavraud, V. N. Coffey, M. O. Chandler, Y. Saito, W. R. Paterson, S. A. Fuselier, R. E. Ergun, R. J. Strangeway, C. T. Russell, B. L. Giles, C. J. Pollock, R. B. Torbert, and J. L. Burch, Nat. Commun. **8**, 14719 (2017).

[32]S. Duan, Z. Liu, and V. Angelopoulos, Chin. Sci. Bull. **57**, 1429 (2012).

[33]N. Kloecker, H. Luehr, A. Korth, and P. Robert, J. Geophys. **57**, 65 (1985).

[34]S. Perraut, O. L. Contel, A. Roux, R. Pellat, A. Korth, Ø. Holter, and A. Pedersen, Geophys. Res. Lett. **27**(14), 4041–4044, https://doi.org/10.1029/2000GL000054 (2000).

[35]G. L. Huang, D.-Y. Wang, D.-J. Wu, H. de Féraudy, D. L. Quéau, M. Volwerk, and B. Holback, J. Geophys. Res. **102**(A4), 7217, https://doi.org/10.1029/96JA02607 (1997).

[36]C. C. Chaston, V. Genot, J. W. Bonnell, C. W. Carlson, J. P. McFadden, R. E. Ergun, R. J. Strangeway, E. J. Lund, and K. J. Hwang, Geophys. Res. Lett. **111**, A03206, https://doi.org/10.1029/2005JA011367 (2006).

[37]C. C. Chaston et al., Geophys. Res. Lett. **41**, 209–215, https://doi.org/10.1002/2013GL058507 (2014).

[38]P. S. Moya, V. A. Pinto, A. F. Vias, D. G. Sibeck, W. S. Kurth, G. B. Hospodarsky, and J. R. Wygant, J. Geophys. Res. Space Phys. **120**, 5504, https://doi.org/10.1002/2014JA020281 (2015).

[39]M. H. Boehm, C. W. Carlson, J. P. McFadden, J. H. Clemmons, and F. S. Mozer, J. Geophys. Res.: Space Phys. **95**, 12157, https://doi.org/10.1029/JA095iA08p12157 (1990).

[40]J.-E. Wahlund, P. Louarn, T. Chust, H. De Feraudy, A. Roux, B. Holback, P.-O. Dovner, and G. Holmgren, Geophys. Res. Lett. **21**, 1831, https://doi.org/10.1029/94GL01289 (1994).

[41]P. Louarn, J. E. Wahlund, T. Chust, H. De Feraudy, A. Roux, B. Holback, P. O. Dovner, A. I. Eriksson, and G. Holmgren, Geophys. Res. Lett. **21**, 1847, https://doi.org/10.1029/94GL00882 (1994).

[42]C. S. Salem, G. G. Howes, D. Sundkvist, S. D. Bale, C. C. Chaston, C. H. K. Chen, and F. S. Mozer, Astrophys. J. Lett. **745**, L9 (2012).

[43]R. P. Sharma and K. V. Modi, Phys. Plasmas **20**, 082305 (2013).

[44]K. V. Modi and R. P. Sharma, Phys. Plasmas **20**, 032303 (2013).

[45]R. P. Sharma, R. Goyal, E. E. Scime, and N. K. Dwivedi, Phys. Plasmas **21**, 042113 (2014).

[46]R. Goyal, R. P. Sharma, and E. E. Scime, Phys. Plasmas **22**, 022101 (2015).

[47]N. Yadav, R. K. Rai, P. Sharma, R. Uma, and R. P. Sharma, Phys. Plasmas **24**, 062902 (2017).

[48]A. Hasegawa and T. Sato, Phys. Chem. Space **16**, 88 (1989).

[49]J. A. Rome and R. J. Briggs, "Stability of sheared electron flow," Phys. Fluids **15**, 796 (1972).

[50]P. J. Catto, M. N. Rosenbluth, and C. S. Liu, Phys. Fluids **16**, 1719 (1973).

[51]G. S. Lakhina and B. T. Tsurutani, J. Geophys. Res. **104**, 279, https://doi.org/10.1029/98JA02724 (1999).

[52]B. D. Fried, "On the mechanism for instability of transverse plasma waves," Technical Report 3, TRW Space Technology Labs Los Angeles, CA, 1959.

[53]H. Momota, Prog. Theor. Phys. **35**, 380 (1966).

[54]K. F. Lee, Phys. Rev. **181**, 453 (1969).

[55]N. Rubab, A. C.-L. Chian, and V. Jatenco-Pereira, J. Geophys. Res. **121**, 1874, https://doi.org/10.1002/2015JA022206 (2016).

[56]G. S. Lakhina, B. T. Tsurutani, H. Kojima, and H. Matsumoto, J. Geophys. Res. **105**, 27791, https://doi.org/10.1029/2000JA900054 (2000).

[57]D. G. Swanson, *Plasma Waves*, Series in Plasma Physics, 2nd ed. (CRC Press, 2003), Eqs. (4.169).